7.1 COMPARISON OF OROGRAPHIC PRECIPITATION IN MAP AND IMPROVE II

Robert A. Houze* and Socorro Medina
University of Washington, Seattle, Washington

1. INTRODUCTION

The Mesoscale Alpine Programme (MAP) was conducted over the European Alps in September-November 1999. During autumn, heavy rains and floods can occur when baroclinic troughs move over the region, and moist air flows from the Mediterranean Sea toward the southern Alps. Dual-polarimetric Doppler and vertically pointing radar data collected during MAP on the Mediterranean side of the Alps provided a unique opportunity to examine orographic precipitation processes. They show that both coalescence and riming occurring at low altitudes in high Froude number flow over the foothills of the Alps are important contributors to the orographic precipitation enhancement in this region (Houze et al. 2001; Medina and Houze 2002).

The question arises whether the orographic precipitation processes seen in MAP are a general characteristic of orographic precipitation enhancement, whenever maritime air flows over a mountain range. The Oregon Cascades, like the Alps, are exposed to a maritime regime of baroclinic waves producing precipitation, which is enhanced over the windward slopes of the mountains. Data collected during the second phase of the Improvement of Microphysical PaRametrization through Observational Verification Experiment (IMPROVE II) conducted over the Oregon Cascades are used to test the generality of the MAP results. This test is possible since the main observational instruments used in the Alps during MAP were also used in the Cascades during IMPROVE II. This paper presents preliminary results from IMPROVE II and compares them with the results of MAP to determine the similarities and differences of orographic precipitation growth mechanisms in baroclinic systems over the Alps and the Oregon Cascades.

2. PRECIPITATION GROWTH MECHANISMS DURING MAP

MAP (Bougeault et al. 2001) was conducted over the Lago Maggiore region (Fig. 1) during autumn, a season that is characterized by a precipitation maximum over the region (Frei and Schaer 1998). This precipitation maximum is produced as southerly, maritime air at low levels, ahead of baroclinic troughs, impinges on the mountain barrier (Massacand et al. 1998). One of such intense trough occurred 19-21 September 2001 (IOP2b) during the Special Observing Period (SOP) of MAP. This storm produced rainfall accumulations >250 mm over some stations on the western slopes of the Lago Maggiore region.

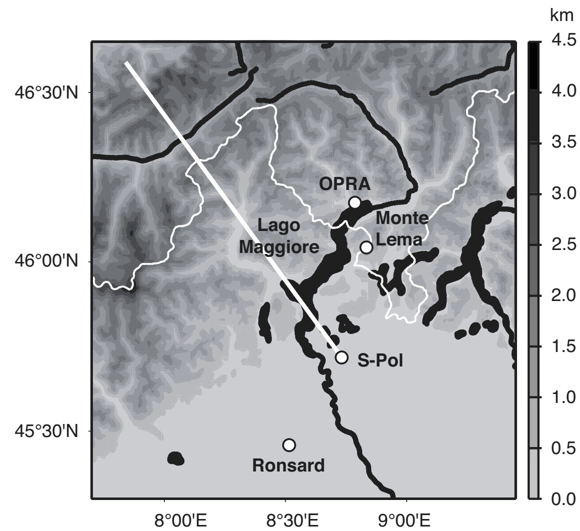

Figure 1. The Lago Maggiore region with bodies of water and MAP radar locations (white dots). The white line shows the location of the cross section shown in Fig. 2.

Figure 1 also shows the location of the MAP radar network in relation to the terrain. The cross section in Fig. 2** shows a 4-hour mean of S-Pol data during IOP2b, illustrating the main precipitation growth mechanisms active during this storm. The cross section (white line in Fig. 1) lies approximately parallel to the low-level wind, and extends from S-Pol, located over the Po Valley, northwestward to the lower Alpine slopes. The S-Pol maximum reflectivity was located over the first peak of the terrain (Fig. 2a). The 0˚C level during this storm was at about 3 km MSL. The maximum reflectivity was located below this level, not very high above the terrain surface. This pattern suggests the importance of low-level coalescence in the precipitation process, as suggested for the Big Thompson flood by Caracena et al. (1979). The radial velocity cross section (Fig. 2b)

* *Corresponding author address:* Professor Robert A. Houze, Jr., University of Washington, Dept. of Atmospheric Sciences, Box 351640, Seattle, WA 98195-1640; email: houze@atmos.washington.edu

** To see color versions of the figures, please visit www.atmos.washington.edu/gcg/MG/PDFs/prep02_houz_comparison.pdf

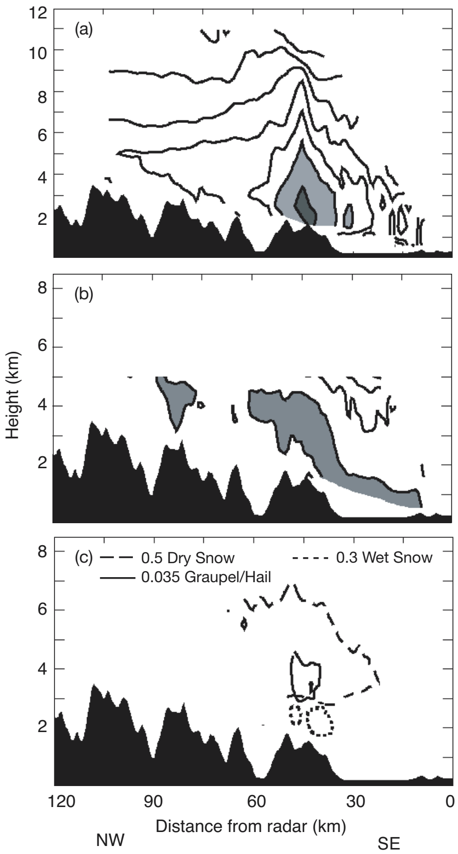

Figure 2. Vertical cross section along the white line in Fig. 1 of S-Pol radar data for 1500-1900 UTC 20 September 1999. (a) Mean reflectivity contoured every 10 dBZ, with dBZ > 42 in dark gray and 32 < dBZ < 42 in light gray. (b) Mean radial velocity contoured every 5 m s^{-1}, with radial velocity > 12 m s^{-1} shaded.

shows a low-level jet that rose abruptly as the airflow encountered the first peak of the topography. Such a dynamical mechanism efficiently transported low-level moisture to higher levels.

Particle-identification algorithms (Vivekanandan et al. 1999; Zeng et al. 2001) were applied to S-Pol dual-polarization radar data. Figure 2c shows frequency of occurrence of hydrometeor types in this cross section during the same 4-hour period. Graupel occurred preferentially above the first major mountain peak, directly above the reflectivity maximum (Fig. 2a). This location coincided with the downwind location where the radial velocity jet reached its maximum altitude directly over the top of the first large peak of the terrain (Fig. 2b). The graupel occurred intermittently at the peak of the rise of the jet and was embedded in a continuously present broad layer of dry snow, which was melting, falling, and turning into a layer of wet snow below. The maximum of graupel occurrence directly over the precipitation maximum seen in the reflectivity suggests that riming of ice particles just above the 0˚C level, and their subsequent fallout and melting may have been another major factor besides coalescence contributing to the reflectivity maximum at lower levels. The low-level jet transported moisture above the 0˚C level, efficiently saturating and condensing cloud liquid water, which was both collected by raindrops below the 0˚C level and accreted by ice particles above this level. This process contributed to the high efficiency of the orographic precipitation in this zone, which allowed the enhanced baroclinic precipitation to fall out and run off on the lower windward slopes.

The low-level upslope flow seen in Fig. 2b was possible because the incident flow was strong and nearly moist neutral. The flow thus had the energy required to rise over the barrier. The precipitation process was further enhanced because the Brunt-Väisälä frequency of the low-level flow was actually slightly negative, so that the strong upslope flow contained local convectively enhanced vertical motion over peaks of the terrain. The high resolution S-band vertically pointing OPRA radar data showed pockets of convective vertical velocity above the reflectivity bright band at the 3-km melting level (Fig. 3a). The black pixels show regions of radial velocity > 2 m s^{-1} upward (Fig. 3b). The radial velocity was not corrected for the fall velocity of the snow, so the air motion was unambiguously moving upward at a

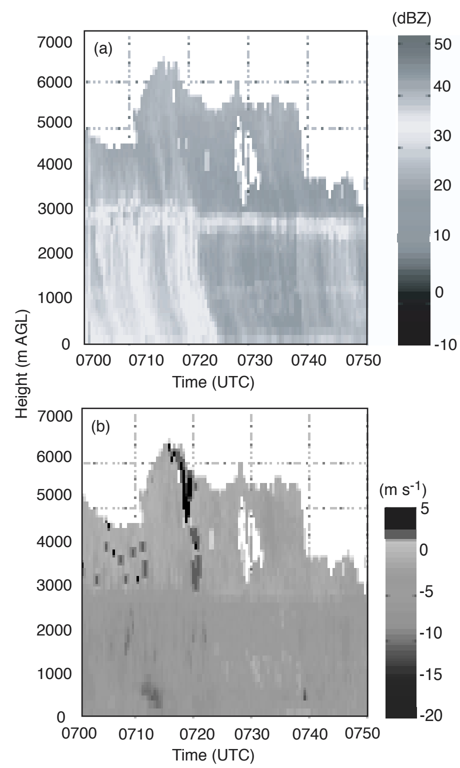

Figure 3. Data from the OPRA S-band vertically pointing radar at Locarno Monti, Switzerland during 0700-0750 UTC 20 September 1999. (a) Reflectivity, (b) radial velocity. The black pixels show regions of radial velocity > 2 m s^{-1} upward.

speed of the order of meters per second. The data from the vertically pointing S-band radar OPRA has provided input for simple bulk microphysical model calculations in which the vertical motion profile is set to be consistent with the cells observed by the vertically pointing S-band radar (Yuter and Houze 2002). These calculations show that coalescence below the bright band and riming just above it are consistent with the updrafts implied by the vertically pointing S-band radar.

3. PRECIPITATION GROWTH MECHANISMS DURING IMPROVE II

IMPROVE II was conducted over the Oregon Cascades (Fig. 4) in November-December 2001 (Hobbs et al. 2002). Its objective was to verify and improve bulk microphysical parametrizations of orographic precipitation in mesoscale models. Since IMPROVE II employed some of the observational facilities that were crucial during MAP, it provided an opportunity to test the generality of the MAP results. In IMPROVE II, the S-Pol radar was located at the base of the foothills of the mountain range, and an S-band vertically pointing radar, operated by NOAA/ETL, was set up in the lower foothills, in the area of coverage of the S-Pol, similar to the deployment of OPRA in MAP (cf. Figs. 1 and 4). In addition, during IMPROVE II, observers stationed near the crest of the Cascades documented particle types reaching the ground. There were also four wind profilers, three sounding sites, and a suite of remote sensing instruments operated by the Pacific Northwest National Lab/Atmospheric Remote Sensing Lab (PARSL) on the lee side of the Cascades.

During IMPROVE II, 16 baroclinic troughs passed over the Cascades producing precipitation. One of these events occurred 13-14 December, producing ~130 mm of precipitation at Little Meadows (Fig. 4). A cross section of S-Pol data approximately in the direction of the low-level wind (white line in Fig. 4) for a 3-hour period during the cold frontal phase of this storm is shown in Fig. 5. The figure shows frequency of occurrence of hydrometeor types calculated by applying the particle-identification algorithms of Vivekanandan et al. (1999) to the S-Pol dual-polarization radar data. Graupel occurred at an altitude of 1.5 km, 10-30 km to the west of S-Pol, where the Cascades start to slope upward (Fig. 4). During this storm, the precipitation measured upstream at Salem in the Willamette Valley (40 mm) was a factor of three less than at the Little Meadows site, only 70 km from Salem in the foothills of the Cascades. Graupel was observed at longitudes corresponding to the zone between Salem and Little Meadows, suggesting that graupel production by riming could have been the mechanism by which the orographic enhancement was achieved. As in MAP, the graupel was located just above the 0˚C level, just below a layer of dry snow and overriding a layer of wet snow (cf. Figs. 2c and 5).

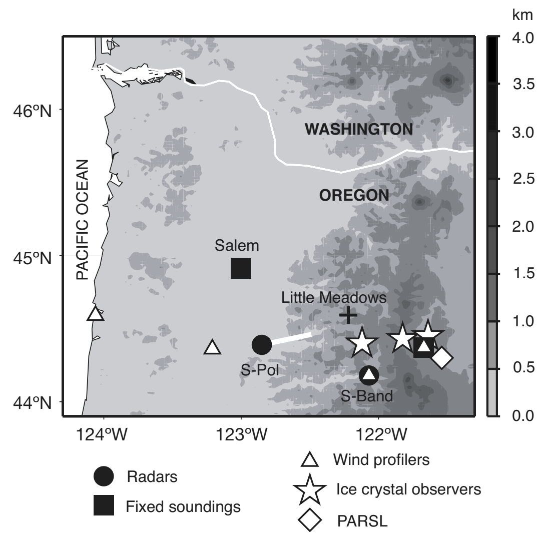

Figure 4. IMPROVE II observational area. Western Oregon topography with locations of observations. The white line shows the location of the cross section shown in Fig. 5.

The vertically pointing S-band radar was located to the southeast and upslope from where the cross section in Fig. 5 ends (Fig. 4). The observed wind speeds during this storm at the 1.5-km level had a southwesterly component of ~15.5 m s^{-1}, implying an advection time of ~1h 15 min from the longitude of the S-Pol to that of the S-band site. A three-hour period of S-band data, lagging 1h 15 min behind the 3-hour period shown in Fig. 5 to allow for advection, shows a continuous deep layer of precipitation with a well-defined bright band, which lowered as the cold air arrived (Fig. 6a). The cold frontal precipitation exhibited embedded con-

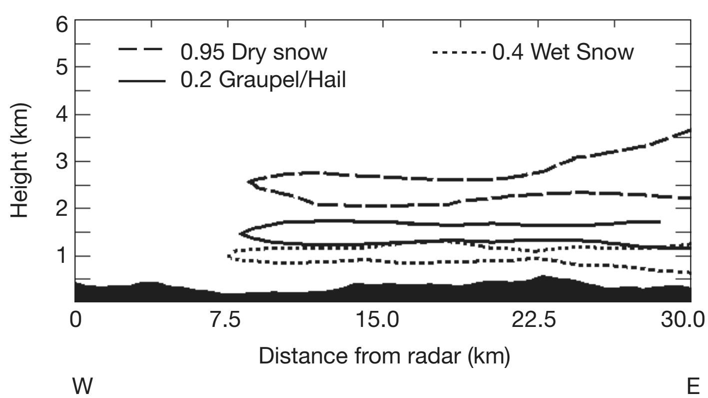

Figure 5. Vertical cross section along the white line in Fig. 4 of S-Pol radar data for 2100-2359 UTC 13 December 2001 of mean frequency of occurrence of particle types identified by polarimetric radar algorithms.

vective cellular structure. The vertically pointing radar Doppler velocity data in the cold frontal region showed upward velocities in these cells (in Fig. 6b black pixels show regions of radial velocity > 0.5 m s^{-1} upward), just above the melting level and above the altitude where the graupel was observed, in a way that resembles the updrafts seen by OPRA during MAP (Fig. 3b).

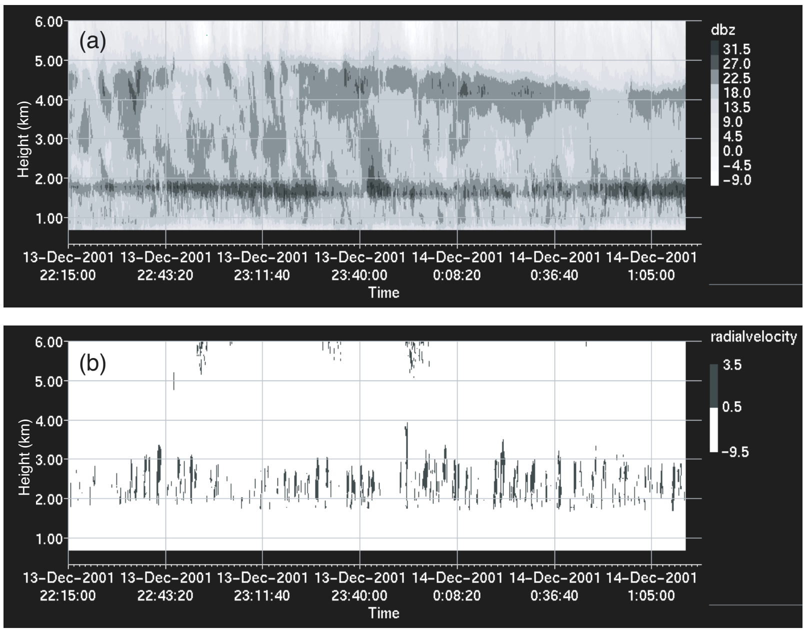

Figure 6. Data from the NOAA/ETL S-band vertically pointing radar, which was located during IMPROVE II at McKenzie Bridge, Oregon. The data shown are for 2215 UTC 13 December - 0115 UTC 14 December 2001. (a) Reflectivity, (b) radial velocity. The black pixels show regions of radial velocity > 0.5 m s^{-1} upward.

4. CONCLUSIONS

Riming appears to play an important role in orographic enhancement of baroclinic precipitation in both the Alps and the Cascades. Over the Alps, strong slightly unstable air impinges on the steep slopes and rises over them, transporting low-level moisture at higher levels and efficiently producing cloud liquid water both above the 0˚C level, promoting riming, and below this level, promoting coalescence. Furthermore, the slight instability promotes convective cell formation that enhances the liquid water production. Over the Cascades, the precipitation was enhanced by a factor of three in a distance of 70 km, just where the terrain begins to slope upward. Particle-identification algorithms detected graupel over this region, making riming a good candidate to explain the precipitation enhancement. Small-scale updrafts, similar to ones seen during MAP, were observed above the layer of graupel. We are continuing to analyze the radial velocity, reflectivity, and polarimetric radar data in both MAP and IMPROVE II to assess the dynamical and microphysical mechanisms that enhance baroclinic precipitation over mountain ranges, with particular attention to the roles of graupel production and warm coalescence over the lower windward slopes.

5. REFERENCES

Bougeault, P., P. Binder, A. Buzzi, R. Dirks, R. A. Houze, Jr., J. Kuettner, R. B. Smith, R. Steinacker, and H. Volkert, 2001: The MAP special observing period. *Bull. Amer. Meteor. Soc.*, **82**, 433-462.

Caracena, F., R. A. Maddox, L. R. Hoxit, and C. F. Chappell, 1979: Mesoanalysis of the Big Thompson storm. *Mon. Wea. Rev.*, **107**, 1-17.

Frei, C., and C. Schaer, 1998: A precipitation climatology of the Alps from high-resolution rain-gauge observations. *Int. J. Climatol.*,**18**, 873-900.

Hobbs, P. V., C. F. Mass, M. T. Stoelinga, J. L. Locatelli, B. A. Colle, N. A. Bond, and R. A. Houze, Jr., 2002: Improvement of microphysical parameterization through observational verification experiments (the IMPROVE project). Proceedings, *11th Conference on Cloud Physics*, Ogden, UT, American Meteorological Society.

Houze, R. A., Jr., C. N. James, and S. Medina 2001: Radar observations of precipitation and airflow on the Mediterranean side of the Alps: Autumn 1998 and 1999. *Quart. J. Roy. Meteor. Soc.*, **127**, 2537-2558.

Massacand, A. C., H. Wernli, and H. C. Davies, 1998: Heavy precipitation on the Alpine southside: An upper-level precursor. *Geophys. Res. Lett.,* **25**, 1435-1438.

Medina, S., and R. A. Houze, Jr., 2002: Air motions and precipitation growth in alpine storms. *Quart. J. Roy. Meteor. Soc.*, special MAP issue, submitted.

Vivekanandan, J., D. S. Zrnic, S. M. Ellis, R. Oye, A. V. Ryzhkov, and J. Straka, 1999: Cloud microphysics retrieval using S-band dual-polarization radar measurements. *Bull. Amer. Meteor. Soc.*, **80**, 381-388.

Yuter, S. E., and R. A. Houze, Jr., 2002: Microphysical modes of precipitation growth determined by S-band vertically pointing radar in orographic precipitation during MAP. *Quart. J. Roy. Meteor. Soc.*, special MAP issue, submitted.

Zeng, Z., S. E. Yuter, R. A. Houze, and D. E. Kingsmill, 2001: Microphysics of the rapid development of heavy convective precipitation. *Mon. Wea. Rev.*, **129**, 1882-1904.